Traveling-wave convection in the presence of a horizontal magnetic field

F. H. Busse and R. M. Clever
Institute of Geophysics and Planetary Physics, University of California at Los Angeles, Los Angeles, California 90024
and Physikalisches Institut, Universität Bayreuth, Universitätsstrasse 30, Postfach 101251,
D-8580 Bayreuth, Federal Republic of Germany
(Received 21 March 1989)

The problem of time-dependent convection flow in a layer heated from below with no-slip boundaries is investigated in the case of electrically conducting fluids permeated by a homogeneous horizontal magnetic field. The Prandtl numbers of 0.1 and 0.025 are considered. Because the onset of oscillations is delayed owing to the presence of the magnetic field and because of the reduced heat transport in the case of traveling-wave convection, the Nusselt number is typically larger in the magnetic case. Convection in the form of symmetric traveling waves becomes unstable with respect to two different types of asymmetric disturbances. The monotonic asymmetric instability is preferred at high magnetic field strength, while the oscillatory asymmetric instability is found in the low-field case. The magnetic field can thus be used as a control parameter to follow the transition from one type of asymmetric wave convection to another.

I. INTRODUCTION

The transition from convection, in the form of steady rolls, to a time-dependent state of oscillating motions, in the form of waves traveling along the axis of the rolls, has always been of special interest to investigators since this transition marks an important step towards the onset of chaotic motion. The onset of oscillations is connected with the occupation of a new degree of freedom of motion in that the vertical vorticity becomes finite, which vanishes for steady rolls. The simplest description of the oscillatory instability is obtained in the limit of vanishing Prandtl number of the fluid in the presence of stress-free boundaries.[1] The analytical theory also indicates that the frequency of oscillations is related to the circulation time of the motion in the convection rolls. In recent years, the finite amplitude properties of traveling-wave convection have been explored. A systematic investigation of those properties as a function of the Prandtl number has been given by Clever and Busse[2] (referred to in the following as CB), in which paper references to related earlier work can be found. In the present paper, this analysis is extended to the case of an electrically conducting fluid that is permeated by a horizontal magnetic field.

Convection in a liquid metal heated from below in the presence of a homogeneous horizontal magnetic field is of special experimental interest. Since the convection rolls become aligned with the direction of the magnetic field, a highly regular pattern of rolls can be obtained.[3] This regularity persists even after the onset of three-dimensional motions in the form of traveling-wave convection. Moreover, the magnetic field strength provides an additional control parameter as a function of which the transition to oscillatory convection and other higher transitions can be varied. A number of important results on transitions to chaotic fluid motion have been obtained by this experimental technique.[3] The problem of traveling-wave convection in the presence of a horizontal magnetic field is also of interest in geophysical and astrophysical applications of convection theory. Convection in the earth's core and in the solar atmosphere is influenced by the presence of magnetic fields. Convection rolls nearly aligned with the direction of the magnetic field appear to occur in the penumbrae of sunspots[4] and the traveling-wave convection and its instabilities may be related to some three-dimensional properties observed in penumbrae.[5]

The onset of the oscillatory instability of steady convection rolls in the presence of a horizontal magnetic field has been computed in an earlier paper,[6] which will be referred to as BC. These results provide the starting values for the finite amplitude analysis, in this paper, of the traveling-wave solutions bifurcating from the steady rolls. Following BC, we shall assume the limit of high magnetic diffusivity λ which is appropriate for experiments in liquid metals. Accordingly, the magnetic Reynolds number is vanishingly small and the main effect of the magnetic field is its stabilizing effect on the onset of the oscillations. The magnetic field also delays the third transition to asymmetric traveling waves described by the critical Rayleigh number R_{III}. There are two different types of this instability, one of which cannot be observed in the absence of a magnetic field unless the Prandtl number becomes very small.

II. MATHEMATICAL FORMULATION OF THE PROBLEM

We consider a horizontal layer of an electrically conducting fluid which is permeated by a homogeneous horizontal magnetic field with the flux density B_0. Using the thickness d of the layer as length scale, d^2/κ as time scale, $\nu\kappa/d^3\gamma g$ as scale for the temperature, and $B_0\kappa/\lambda$ as scale for the magnetic field, we introduce a nondimensional description of the problem. The symbols κ, ν, γ, g, and λ denote the thermal diffusivity, the kinematic

viscosity, the coefficient of thermal expansion, the acceleration of gravity, and the magnetic diffusivity, respectively. Since the magnetic field $\mathbf{B}$ and the velocity field $\mathbf{u}$ in the Boussinesq approximation are solenoidal vector fields, the general representation

$$\mathbf{u}=\nabla\times(\nabla\times\hat{\mathbf{k}}\phi)+\nabla\times\hat{\mathbf{k}}\psi+U\hat{\mathbf{i}}\equiv\delta\phi+\varepsilon\psi+U\hat{\mathbf{i}}\ , \quad (1a)$$

$$\mathbf{B}=\frac{\lambda}{\kappa}\hat{\mathbf{i}}+\delta h+\varepsilon g\ , \quad (1b)$$

can be used where $\hat{\mathbf{k}}$ and $\hat{\mathbf{i}}$ denote the unit vectors in the vertical and in the magnetic field direction, respectively. We shall use a Cartesian system of coordinates with the x and z coordinates in directions of $\hat{\mathbf{i}}$ and $\hat{\mathbf{k}}$. Since we require that ϕ, ψ, h and g are bounded functions whose averages over the x-y plane vanish, the possibility of a mean flow must be described separately. In writing (1) we have anticipated that a mean flow can occur only in the x direction and that only fluctuating modifications of the imposed magnetic field can occur.

By taking the z components of the curl and of the curl squared of the equations of motion, we obtain two equations for ϕ and ψ. Similarly, by taking the z components of the equation of magnetic induction and of its curl, two equations for h and g are obtained. These equations must be supplemented by the heat equation for the deviation θ of the temperature field from the basic state of pure conduction and by the horizontal average of the x component of the equation of motion. The latter average will be indicated by a bar. The six equations assume the following form after all terms with κ/λ as a factor have been neglected since we are assuming the limit of high magnetic diffusivity:

$$\nabla^4\Delta_2\phi-\Delta_2\theta+Q\hat{\mathbf{i}}\cdot\nabla\Delta_2\nabla^2 h = P^{-1}\left[\frac{\partial}{\partial t}\nabla^2\Delta_2\phi+\delta\cdot(\mathbf{u}\cdot\nabla\mathbf{u})\right]\ , \quad (2a)$$

$$\nabla^2\Delta_2\psi+Q\hat{\mathbf{i}}\cdot\nabla\Delta_2 g=P^{-1}\left[\frac{\partial}{\partial t}\Delta_2\psi+\varepsilon\cdot(\mathbf{u}\cdot\nabla\mathbf{u})\right]\ , \quad (2b)$$

$$\nabla^2\theta-R\Delta_2\phi=\frac{\partial}{\partial t}\theta+\mathbf{u}\cdot\nabla\theta\ , \quad (2c)$$

$$\nabla^2\Delta_2 h+\hat{\mathbf{i}}\cdot\nabla\Delta_2\phi=0\ , \quad (2d)$$

$$\nabla^2\Delta_2 g+\hat{\mathbf{i}}\cdot\nabla\Delta_2\psi=0\ , \quad (2e)$$

$$\frac{\partial^2}{\partial z^2}U-P^{-1}\frac{\partial}{\partial t}U=-P^{-1}\frac{\partial}{\partial z}[\overline{\Delta_2\phi(\partial_{xz}\phi-\partial_y\psi)}]+\eta\ , \quad (2f)$$

where Δ_2 denotes the horizontal Laplacian, $\Delta_2\equiv\nabla^2-(\hat{\mathbf{k}}\cdot\nabla)^2$, the bar indicates the average over the x-y plane, and where the Rayleigh, Prandtl, and Chandrasekhar numbers are defined by

$$R\equiv\gamma(T_2-T_1)gd^3/\kappa\nu,\quad P\equiv\nu/\kappa,\quad Q\equiv B_0^2d^2/\rho_0\mu\nu\lambda\ , \quad (3)$$

respectively. We have also introduced the constant η, which represents the possibility of a constant pressure gradient in the x direction as will be discussed below in more detail. The temperatures T_1 and T_2, with $T_1<T_2$, are prescribed at the upper and lower rigid boundaries of the layer, and ρ_0 and μ denote the density and the magnetic permeability of the fluid, respectively. For a more detailed derivation of Eqs. (2), see BC.

The high magnetic diffusion limit offers the advantage that the variable h can be eliminated immediately from the problem by the use of Eq. (2d) in Eq. (2a). The elimination of the other magnetic field variable g is not quite as straightforward, but Eq. (2e) can be solved most readily if electrically insulating rigid top and bottom boundaries are used. Since we also require that the temperature perturbations vanish at the boundaries, the boundary conditions become

$$\phi=\frac{\partial}{\partial z}\phi=\psi=g=\theta=0\ \text{ at } z=\pm\tfrac{1}{2}\ . \quad (4)$$

It is well known that convection sets at the critical Rayleigh number R_c in the form of rolls aligned with the direction of the horizontal magnetic field.[7] For these rolls, ψ and g vanish identically and the nature of the magnetic boundary conditions is irrelevant. But the instabilities of the rolls are influenced by the magnetic boundary conditions. For the moderate field strength considered in this paper it is not likely, however, that the dominant role of the oscillatory instability in low Prandtl number fluids found by BC will be much affected by different magnetic boundary conditions.

In the present paper, the traveling-wave convection evolving from the oscillatory instability superimposed onto the steady rolls will be investigated. For this purpose, the dependent variables ϕ, ψ, θ, and U are expanded into complete systems of orthogonal functions satisfying the appropriate boundary conditions,

$$\phi=\sum_{l,m,n}[\hat{a}_{lmn}\cos m\alpha_y(y-ct)+a_{lmn}\sin m\alpha_y(y-ct)]\begin{Bmatrix}\sin l\alpha_x x\\ \cos l\alpha_x x\end{Bmatrix}g_n(z) \equiv\sum_{l,m,n}(\hat{a}_{lmn}\hat{\Phi}_{lmn}+a_{lmn}\Phi_{lmn})\ , \quad (5a)$$

$$\theta=\sum_{l,m,n}[\hat{b}_{lmn}\cos m\alpha_y(y-ct)+b_{lmn}\sin m\alpha_y(y-ct)]\begin{Bmatrix}\sin l\alpha_x x\\ \cos l\alpha_x x\end{Bmatrix}\sin n\pi(z+\tfrac{1}{2}) \equiv\sum_{l,m,n}(\hat{b}_{lmn}\hat{\Theta}_{lmn}+b_{lmn}\Theta_{lmn})\ , \quad (5b)$$

$$\psi=\sum_{l,m,n}[\hat{c}_{lmn}\cos m\alpha_y(y-ct)+c_{lmn}\sin m\alpha_y(y-ct)]\begin{Bmatrix}\cos l\alpha_x x\\ \sin l\alpha_x x\end{Bmatrix}\times\sin(n-1)\pi(z+\tfrac{1}{2}) \equiv\sum_{l,m,n}(\hat{c}_{lmn}\hat{\Psi}_{lmn}+c_{lmn}\Psi_{lmn})\ , \quad (5c)$$

$$U=\sum_n U_n\sin n\pi(z+\tfrac{1}{2})\ , \quad (5d)$$

where the indices l and m run through all non-negative integers, while n runs through all positive integers. The functions $g_n(z)$ have been introduced by Chandrasekhar[8] and have been used in earlier work by the authors.[9] Following CB, the upper functions inside the wavy brackets must be chosen for odd m, the lower functions for even m. In the case of the traveling-wave solution bifurcating from the steady rolls, all coefficients with odd $l+n$ vanish, which reduces the numerical effort considerably.

For a given expression (5c) for ψ, Eq. (2e) can be solved readily by

$$g=\sum_{lmn}\left[\hat{c}_{lmn}\frac{\partial}{\partial x}\hat{\Psi}_{lmn}+c_{lmn}\frac{\partial}{\partial x}\Psi_{lmn}\right]\times[m^2\alpha_y^2+l^2\alpha_x^2+(n-1)^2\pi^2]^{-1}\,, \tag{6}$$

which satisfies the condition $g=0$ at $z=\pm\frac{1}{2}$. After inserting the expansion (5) and (6) into Eqs. (2a)–(2c), multiplying these equations with the functions $\hat{\Phi}_{ijk}$, Φ_{ijk}, $\hat{\Theta}_{ijk}$, Θ_{ijk}, $\hat{\Psi}_{ijk}$, and Ψ_{ijk}, and averaging them over the fluid layer, we obtain a system of nonlinear algebraic equations for the unknown coefficients $\hat{a}_{ijk}$, etc. These equations are not given here since they are similar to those used in earlier work.[10] The system of algebraic equations is solved by the Newton-Raphson method after the system has been truncated. As in CB87, we neglect all coefficients $\hat{a}_{ijk}$, etc., and corresponding equations whenever the subscripts satisfy the truncation condition

$$i+j+k>N_T\,. \tag{7}$$

By considering the convergence with increasing N_T of sensitive properties of the solution, such as the convective heat transport, we can check the quality of the approximation. Usually an approximate solution is regarded satisfactory if the heat transport does not change by more than a few percent when N_T is replaced by N_T-1.

Because of the invariance of the problem with respect to a translation in the x direction, the phase of the traveling wave can be fixed without loss of generality by requiring that the coefficient a_{111} vanishes. This procedure provides an extra equation which is just what is needed to determine the phase speed c. From the form (5) of the solution, it is clear that a finite Reynolds stress in the x direction can exist, but it always vanishes in the y direction as we have anticipated earlier. In solving Eq. (2f) we distinguish two cases. In small aspect ratio layers it is reasonable to assume that side walls inhibit a mean horizontal fluid flow. A pressure gradient will arise opposing the mean flow such that the integral of U over z vanishes. this constraint will diminish as the aspect ratio increases, and for very large aspect ratios the mean pressure gradient η can be neglected. We thus consider two limiting cases: (i) restricted case:

$$\eta \text{ is chosen such that } \int_{-1/2}^{+1/2}U\,dz=0 \text{ is satisfied}\,, \tag{8a}$$

(ii) unrestricted case:

$$\eta=0\,. \tag{8b}$$

As will be evident from the results to be discussed in the following, the differences between the two cases are not very large. The effect of the mean flow tends to vanish when the Prandtl number becomes of the order unity or larger. For the small Prandtl number considered in this paper, the mean flow is not negligible, however. Unfortunately, this component of the velocity field had been neglected originally and the small Prandtl number results of CB are slightly in error for this reason. Corrected results are given in a recent paper[11] in which the influence of a vertical magnetic field has been considered.

III. TRAVELING-WAVE CONVECTION

When traveling-wave solutions of the form (5) for different values of R, Q, and P are generated and compared, the most remarkable property is their general similarity. Their properties depend primarily on the supercritical Rayleigh number $R-R_{\rm II}$. The Rayleigh number $R_{\rm II}$ for onset of oscillations, of course, varies strongly with Q and P; but there is little indication for separate influences of the Prandtl number or of the magnetic field. We thus show only two figures, namely, Figs. 1 and 2, depicting some typical properties of the

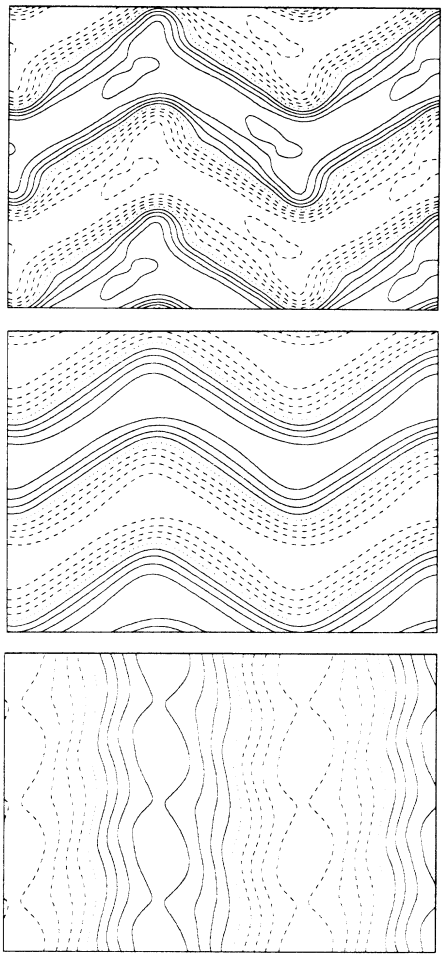

FIG. 1. Traveling-wave convection with $R=3500$, $Q=30$, $\alpha_x=2.1$, and $\alpha_y=2.9$ in the case $P=0.025$ with restricted mean flow. The top (bottom) picture shows lines of constant vertical velocity (toroidal stream function ψ) in the plane $z=0$. The middle picture gives lines of constant $\int_{-1/2}^{1/2}\theta\,dz$. Dashed lines indicate negative values.

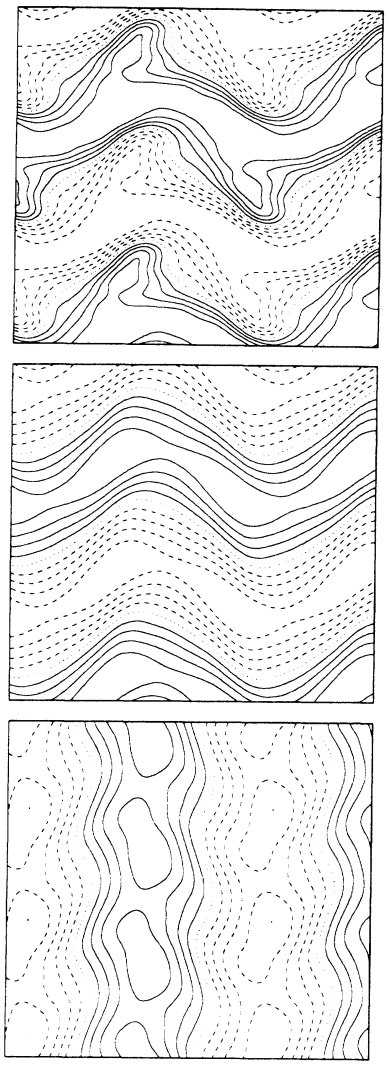

FIG. 2. Same as Fig. 1 in the case $R=10\,500$, $Q=100$, $\alpha_x=2.5$, and $\alpha_y=2.6$ for $P=0.1$.

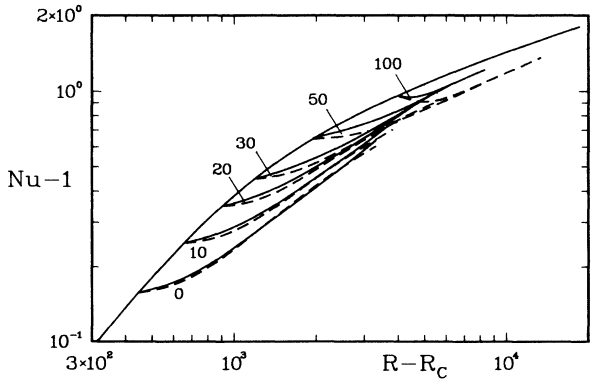

FIG. 3. Nusselt number as function of the supercritical Rayleigh number for two-dimensional rolls ($\alpha_y=2.6$) and for traveling-wave convection for different values of Q (as indicated) for $P=0.1$. In the latter case, solid lines correspond to unrestricted mean flow conditions, dashed lines to restricted mean flow. The values for α_x are the same ones as given in Table I.

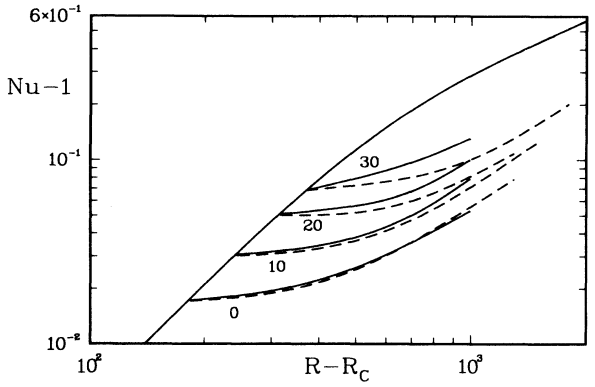

FIG. 4. Same as Fig. 3, but for $P=0.025$ with $\alpha_y=2.9$ and values of α_x as indicated in Table II.

traveling-wave solution. As R is increased beyond R_{II} the waves retain their sinusoidal shape at first. Later, higher harmonics become strongly noticeable as in the case of Figs. 1 and 2. The amplitude of the distortion appears to saturate and a zig-zagging form consisting of nearly straight roll-like segments is achieved in the low-Q cases as shown in Fig. 1. Higher values of Q seem to promote some phases shifts between different components of the wave solution and the wave shape is more rounded as seen in Fig. 2. Because of the low Prandtl number, the amplitude of the wave in the temperature field is smaller than in the case of the vertical velocity field and the small scale feature are damped by the high diffusion of the temperature field.

Of special interest in the comparison between theory and experimental results is the influence of the magnetic field on the heat transport and on the frequency of oscillations. The stabilizing influence of the magnetic field is clearly evident in Figs. 3 and 4, which show the Nusselt number for two different Prandtl number. As has already

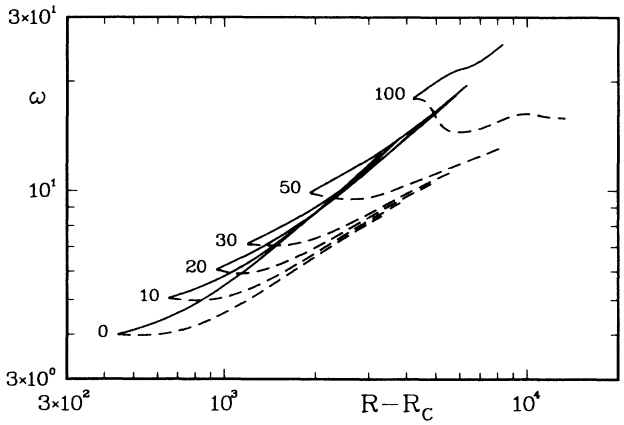

FIG. 5. Frequency $\omega=\alpha_x c$ of traveling-wave convection as a function of the supercritical Rayleigh number for different values of Q in the case $P=0.1$. As before, solid lines correspond to unrestricted mean flow, while dashed lines indicate restricted mean flow and the values of α_x are given in Table I.

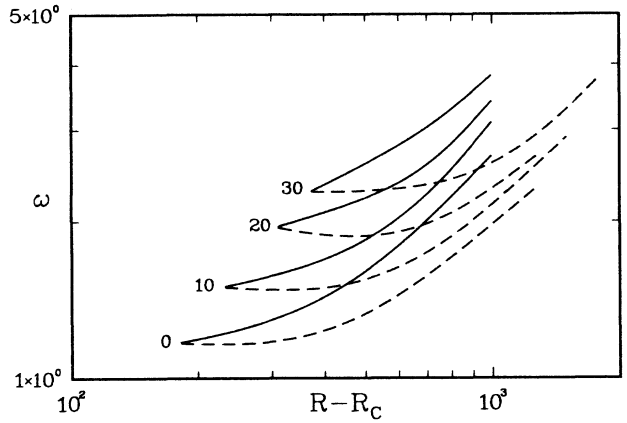

FIG. 6. Same as Fig. 5, but in the case $P=0.025$ with values of α_x given in Table II.

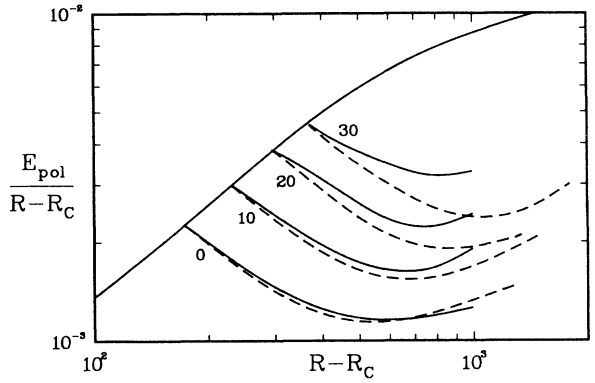

FIG. 8. Same as Fig. 7, but in the case $P=0.25$ with the values of α_x and α_y of Table II.

been emphasized by CB, traveling-wave convection becomes less efficient in comparison to roll convection in transporting heat as the Prandtl number decreases below unity. The application of a horizontal magnetic field can thus increase the convective heat transport by a factor of 1.5 in the case $P=0.1$, but by as much as a factor of 5 in the case $P=0.025$, as is evident from Figs. 3 and 4. It is remarkable that curves of the traveling-wave solutions for different values of Q appear to converge. The strength of the magnetic field thus seems to have little influence once the amplitude of the waves reaches a saturation level.

This convergence for different values of Q is also seen in the frequencies of oscillation plotted in Figs. 5 and 6. Since the frequency is roughly proportional to the circulation velocity of the rolls, the frequency at the onset of oscillatory instability increases with Q just as R_{II} increases. For a while, the frequency changes very little as the Nusselt number stagnates with increasing Rayleigh number. Together with the heat transport, the frequency resumes its growth as it approaches the curve for vanishing Q.

The property of stagnation also appears in the plots of the kinetic energy of the poloidal component of the velocity field which are given in Figs. 7 and 8. This energy is defined by

$$E_{\text{pol}} \equiv \tfrac{1}{2}\langle |\nabla\times(\nabla\times\hat{\mathbf{k}}\phi)|^2\rangle \ , \tag{9a}$$

and gives a measure of the strength of the vertical velocity. By contrast, the toroidal kinetic energy

$$E_{\text{tor}} \equiv \tfrac{1}{2}\langle |\nabla\times\hat{\mathbf{k}}\psi|^2\rangle \tag{9b}$$

measures the strength of the toroidal component, which

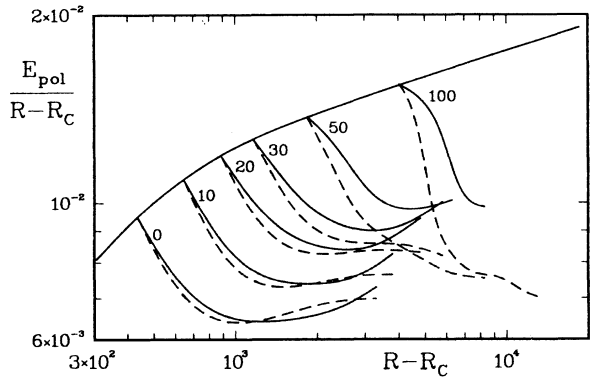

FIG. 7. Kinetic energy of roll convection and the kinetic energy of the poloidal component of the traveling-wave convection velocity field as function of the supercritical Rayleigh number for different values of Q in the case $P=0.1$. Solid lines indicate unrestricted mean flow, dashed lines describe the case of restricted flow. The wave numbers α_x and α_y are those of Table I.

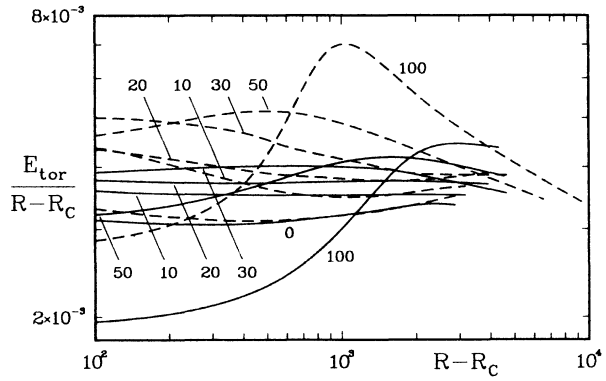

FIG. 9. Kinetic energy E_{tor} of the toroidal component of the traveling-wave velocity field as function of $R-R_{\text{II}}$ for different values of Q in the case $P=0.1$. Solid (dashed) lines indicate unrestricted (restricted) mean flow. The wave number α_x and α_y are given in Table I.

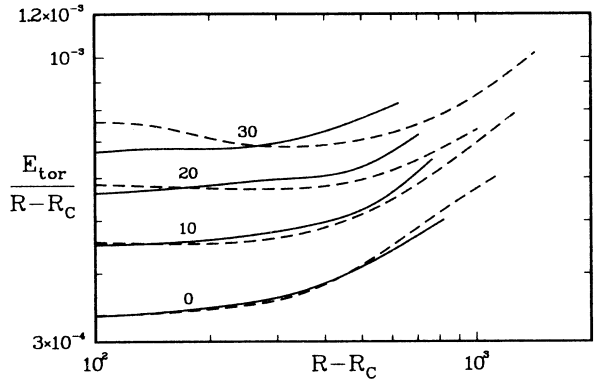

FIG. 10. Same as Fig. 9, but for $P=0.025$ with wave numbers α_x and α_y as given in Table II.

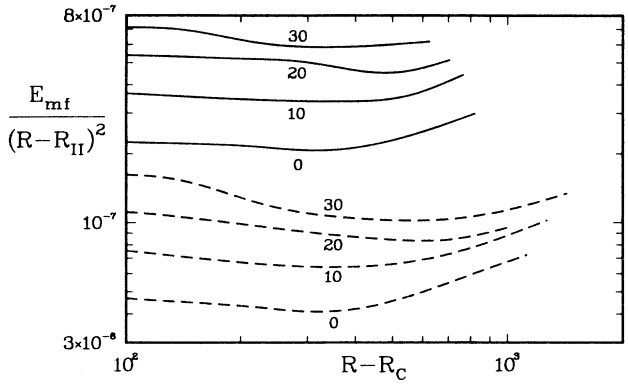

FIG. 12. Same as Fig. 11, but for $P=0.025$.

is introduced by the oscillatory instability. The angular brackets in expressions (9) indicate the average over the fluid layer. As the amplitude of the oscillations grows, the toroidal component grows while the poloidal energy hardly changes, according to Figs. 7 and 8, or actually decreases as in the case $Q=100$ of Fig. 7. Since the toroidal component of motion does not contribute to the heat transport nor does it influence the frequency, these latter quantities resemble the evolution of the poloidal component of motion.

Figures 9 and 10 demonstrate that E_{tor} grows proportional with $R-R_{\text{II}}$, at least for a finite interval beyond the Rayleigh number R_{II} for the onset of oscillations. The constant of proportionality involves the poloidal component of motion and thus increases with Q. Ultimately the curves for different values of Q converge again leading to the impression that the traveling waves are independent of Q for sufficiently high Rayleigh numbers. This impression is confirmed by the evolution of the shape of the waves as we have mentioned above.

In Figs. 3–10, both cases with a restricted mean flow, as well as those with an unrestricted mean flow, have been plotted. As expected, the main effect of the mean

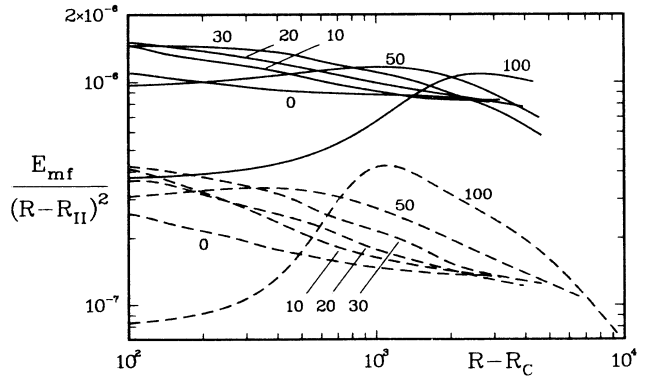

FIG. 11. Kinetic energy of the mean flow, E_{mf}, as a function of $R-R_{\text{II}}$ for different values of Q in the case $P=0.1$. Solid (dashed) lines indicate unrestricted (restricted) mean flow.

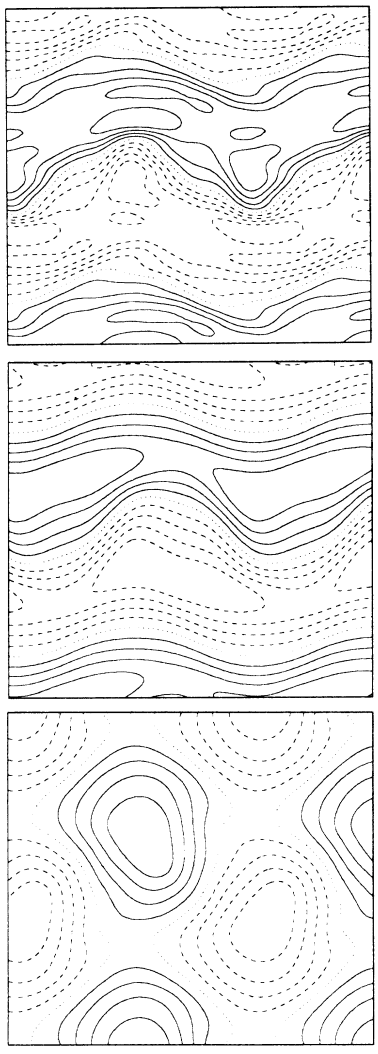

FIG. 13. Asymmetric traveling-wave convection for $R=12\times10^3$, $Q=100$, $P=0.1$, $\alpha_x=2.5$, and $\alpha_y=2.9$.

TABLE I. Rayleigh numbers R_{II} for the onset of symmetric traveling waves and R_{III} for the onset of asymmetric instabilities in the case $P=0.1$, $\alpha_y=2.6$ for different values of Q. The Rayleigh number R_{III} is given for the monotonic, as well as for the oscillating asymmetric instability, and both, restricted (r) and unrestricted (u), mean flow conditions are considered.

			Monotonic asymmetric I		Oscillating asymmetric I			
Q	α_x	R_{II}	$R_{III}(r)$	$R_{III}(u)$	$R_{III}(r)$	$\sigma_i(r)$	$R_{III}(u)$	$\sigma_i(u)$
0	2.2	2145		3605	2707	4.39	2801	5.02
10	2.1	2352		3754	3092	5.43	3274	6.41
20	2.0	2596	4513	4006	3529	6.47	3882	7.92
30	2.0	2879	4785	4359	3988	7.58	4594	9.73
50	2.1	3539	5184	5105	5085	10.03	7869	17.72
100	2.5	5684	6567	7329	9780	17.48		

flow conditions is seen in the plots of the frequency of oscillation, since the unrestricted mean flow is directed in the direction of the traveling waves. But the amplitude of the mean flow is rather small, as is evident from Figs. 11 and 12, where its kinetic energy has been plotted. Since the mean flow is generated by the Reynolds stress associated with the fluctuating component of the traveling waves, its kinetic energy grows approximately like $(R-R_{II})^2$. As R increases, the mean flow kinetic energies converge as expected. But while the growth rate decreases typically (with increasing Rayleigh number) in the case $P=0.1$, an increase of the rate of growth is noticeable for $P=0.025$. Before this effect becomes significant with increasing Rayleigh number, however the symmetric traveling waves discussed in this section become unstable.

IV. TRANSITION TO ASYMMETRIC TRAVELING WAVES

The analysis of the stability of symmetric traveling-wave convection with respect to three-dimensional infinitesimal disturbances will not be discussed here in detail since it follows closely the analysis described in earlier work.[2] Because the horizontal periodicity interval of convection flows described in Sec. III is relatively large, we do not expect wavelength changing disturbances to be important. We thus shall restrict the attention to those disturbances that fit the periodicity cell described by the basic wave numbers α_x and α_y. This restriction has the advantage that the symmetry properties of the stability equations can be used to reduce the computational work.

As has been pointed out in Sec. II, the symmetric traveling-wave convection is described by the subset of the general representation (5) for which the coefficients with odd $l+n$ vanish and for which the upper (lower) functions in the curly brackets must be chosen for odd (even) m. Four classes of disturbances are possible for which either none, or one, of both of these symmetries are changed into the opposite one. Otherwise the solutions of the stability equations have the same form as the symmetric traveling-wave solution (5) except for the extra factor $\exp\{\sigma t\}$.

In the parameter regime of interest only those disturbances which exhibit the opposite parity with respect to both symmetries of the symmetric traveling waves yield a positive real part of the growth rate σ. There are two different kinds of instability, a monotonic instability with vanishing imaginary part σ_i of the growth rate and an oscillatory instability with $\sigma_i \neq 0$. The latter type of instability has been found in the nonmagnetic case. But the monotonic instability becomes preferred as the strength of the horizontal magnetic field increases according to Tables I and II.

The property that an imposed magnetic field favors the onset of the monotonic asymmetric instability is peculiar to the case of a horizontal field direction. While a vertical magnetic field plays a role, which is in many respects similar to that of a horizontal magnetic field, it does not seem to give rise to the monotonic asymmetric instability, at least not for Prandtl numbers $P \geq 0.025$. Both asymmetric instabilities give rise to relatively small modifications of symmetric traveling-wave convection. In Fig. 13 a plot is shown of finite-amplitude asymmetric traveling-wave convection induced by the monotonic instability. As in the case of symmetric traveling-wave convection, the pattern remains steady with respect to the appropriately moving frame of reference.

The case of the finite-amplitude mode of convection in-

TABLE II. Same as Table I but in the case $P=0.025$, $\alpha_y=2.9$.

			Monotonic asymmetric I		Oscillating asymmetric I	
Q	α_x	R_{II}	$R_{III}(r)$	$R_{III}(u)$	$R_{III}(r)$	$\sigma_i(r)$
0	2.2	1883	2703		2482	1.55
10	2.1	1936	2679	2623	2679	1.97
20	2.1	1994	2693	2627	2783	2.29
30	2.1	2076	2727		2875	2.69

duced by the oscillatory asymmetric instability is more difficult to analyze since the time-dependent basic equations must be solved. As has been discussed in Ref. 11, this instability leads double-frequency traveling-wave convection at Prandtl numbers of the order unity or to standing oscillations at lower Prandtl numbers.

V. CONCLUDING REMARKS

The opportunities offered by the additional control parameter provided by the strength of the magnetic field in convection experiments with electrically conducting fluids have long been recognized by Libchaber and coworkers.[3] Unfortunately, the rather high values of Q and the small aspect ratios of the convection boxes employed in those experiments make it difficult to obtain a quantitative comparison between theory and measurements. In qualitative aspects general agreement is found, however.

The shift of the onset of the oscillatory instability towards higher Rayleigh number with increasing field strength is the most obvious feature and can easily be understood by the tension provided by the magnetic field lines. More surprising is the property of the asymptotic convergence of the convective heat transport of symmetric traveling-wave convection for different values of Q. It appears that the inhibiting influences of the Lorentz force on the toroidal component of the velocity field and on the x-dependent component of the poloidal velocity field lead to compensating effects on the heat transport. The experimental data also show a convergence of the heat transport for different values of Q, but this occurs in a different regime after the convection flow has become chaotic.

A typical feature exhibited by the experiments is the decrease of the frequency after the onset of traveling-wave convection. The measured data[12] resemble closely the theoretical curves in Fig. 6 in this respect. On the other hand, the theoretical computations have shown no indication for a subcritical onset of traveling-wave convection as observed in the experiment.[12] This phenomenon seems to be connected with the finite size of the experimental convection box, which leads to a considerable contribution from a standing-wave component.[12] While the semianalytical theory of Fauve *et al.*[13] predicts a subcritical onset of traveling waves for low values of α_y for $Q=0$, this phenomenon has not been found in our numerical computations at vanishing or low values of Q.

The stabilizing influence of a horizontal magnetic field on the onset of traveling waves will allow eventually the experimental study of inertial convection, which manifests itself in a large increase of the convective heat transport at supercritical Rayleigh numbers. In numerical computations[14] the flywheel character of the two-dimensional convection rolls becomes well established at low Prandtl numbers. But the experiments which have been carried out with sufficiently high magnetic field strength have not provided the heat flux data for a comparison with the theoretical data.

ACKNOWLEDGMENTS

The research reported in this paper has been supported by the Atmospheric Sciences Section of the National Science Foundation.

[1]F. H. Busse, J. Fluid Mech. **52**, 97 (1972).
[2]R. M. Clever and F. H. Busse, J. Fluid Mech. **176**, 403 (1987).
[3]A. Libchaber, S. Fauve, and C. Laroche, Physica **7D**, 73 (1983); S. Fauve, C. Laroche, A. Libchaber, and B. Perrin, Phys. Rev. Lett. **52**, 1774 (1984).
[4]R. R. Danielson, Astrophys. J. **134**, 275 (1961).
[5]For a new mechanism for the Evershed effect, see F. H. Busse, in *The Role of Fine-Scale Magnetic Fields on the Structure of the Solar Atmosphere,* edited by E. H. Schroeter, M. Vazquez, and A. Wyller (Cambridge University Press, Cambridge, England, 1988).
[6]F. H. Busse and F. M. Clever, J. Mec. Theor. Appl. **2**, 495 (1983).
[7]S. Chandrasekhar, *Hydrodynamic and Hydromagnetic Stability* (Clarendon, Oxford, England, 1961).
[8]See Ref. 7, p. 635.
[9]R. M. Clever and F. H. Busse, J. Fluid Mech. **65**, 625 (1974).
[10]F. H. Busse and H. Frick, J. Fluid Mech. **150**, 451 (1985).
[11]R. M. Clever and F. H. Busse, J. Fluid Mech. **201**, 507 (1989).
[12]A. Chiffaudel, B. Perrin, and S. Fauve, Phys. Rev. A **34**, 2761 (1989).
[13]S. Fauve, E. W. Bolton, and M. E. Bracket, Physica **29D**, 202 (1987).
[14]R. M. Clever and F. H. Busse, J. Fluid Mech. **102**, 61 (1981).